THE JOURNAL OF BIOLOGICAL CHEMISTRY VOL. 285, NO. 13, pp. 9604–9615, March 26, 2010

Fat-specific Protein 27 Undergoes Ubiquitin-dependent Degradation Regulated by Triacylglycerol Synthesis and Lipid Droplet Formation*[S]

Received for publication, July 14, 2009, and in revised form, January 19, 2010 Published, JBC Papers in Press, January 20, 2010, DOI 10.1074/jbc.M109.043786

Zongqian Nian[‡1], **Zhiqi Sun**[‡1], **Luxin Yu**[§1], **Shen Yon Toh**[¶], **Jianli Sang**[§], **and Peng Li**[‡2]

From the [‡]*Protein Science Laboratory of Ministry of Education, School of Life Sciences, Tsinghua University, Beijing 100084, China, the* [§]*College of Life Sciences, Beijing Normal University, Beijing 100875, China, and the* [¶]*Institute of Molecular and Cell Biology, 138673 Singapore*

The fat-specific protein 27 (Fsp27), a protein localized to lipid droplets (LDs), plays an important role in controlling lipid storage and mitochondrial activity in adipocytes. *Fsp27*-null mice display increased energy expenditure and are resistant to high fat diet-induced obesity and diabetes. However, little is known about how the Fsp27 protein is regulated. Here, we show that Fsp27 stability is controlled by the ubiquitin-dependent proteasomal degradation pathway in adipocytes. The ubiquitination of Fsp27 is regulated by three lysine residues located in the C-terminal region. Substitution of these lysine residues with alanines greatly increased Fsp27 stability and enhanced lipid storage in adipocytes. Furthermore, Fsp27 was stabilized and rapidly accumulated following treatment with β-agonists that induce lipolysis and fatty acid re-esterification in adipocytes. More importantly, Fsp27 stabilization was dependent on triacylglycerol synthesis and LD formation, because knockdown of diacylglycerol acyltransferase in adipocytes significantly reduced Fsp27 accumulation in adipocytes. Finally, we observed that increased Fsp27 during β-agonist treatment preferentially associated with LDs. Taken together, our data revealed that Fsp27 can be stabilized by free fatty acid availability, triacylglycerol synthesis, and LD formation. The stabilization of Fsp27 when free fatty acids are abundant further enhances lipid storage, providing positive feedback to regulate lipid storage in adipocytes.

Cell death-inducing DNA fragmentation factor-45-like effector (Cide) proteins, including Cidea, Cideb, and fat-specific protein 27 (Fsp27,[3] also known as Cidec in humans), are a family of proteins shown to play critical roles in controlling metabolism homeostasis (1). Our previous work demonstrated that mice with a deficiency in *Cidea* or *Cideb* have higher energy expenditure and enhanced insulin sensitivity and are resistant to high fat diet-induced obesity and diabetes (2, 3). Fsp27 is enriched in adipocytes, in both white adipose tissue and brown adipose tissue (2, 4). The Fsp27 protein is detected in the lipid droplet (LD)-enriched fraction (5), and its overexpression can promote triacylglycerol (TAG) storage (6, 7). Interestingly, Fsp27 and Cidea mRNAs have also been detected in fatty livers, where an excess amount of lipids accumulate and large LDs form (8–10). More recently, Fsp27 was demonstrated to be a direct mediator of peroxisome proliferator-activated receptor γ-dependent hepatic steatosis (10). In accordance with a role for Fsp27 in LD formation, *Fsp27* deficiency results in dramatically reduced white adipose tissue deposits and the acquisition of a brown fat-like morphology in these white adipose tissues, which is characterized by the appearance of smaller LDs and increased mitochondrial size and activity (11, 12). Furthermore, both *Fsp27*-deficient and *Fsp27/leptin* double-deficient mice display improved insulin sensitivity and lean phenotype (12). Except for one study showing that Cidea is degraded through the ubiquitin-mediated proteasomal pathway in adipocytes (13), little is known about the regulation of the Cide family proteins on the post-translational level, particularly about the physiological conditions that may play roles in modulating their stability.

Here, we show that endogenous Fsp27 is a highly unstable protein in adipocytes and heterologous cells when ectopically expressed. Its stability is controlled by the ubiquitin-dependent proteasomal pathway. Detailed analyses revealed that three lysine residues in the C-terminal region serve as the ubiquitin acceptor sites. Importantly, we observed that the stability of Fsp27 can be controlled by the β-agonist isoproterenol (Iso), which stimulates lipolysis, and is directly influenced by TAG synthesis and nascent LD formation in adipocytes.

EXPERIMENTAL PROCEDURES

Plasmid Construction, Antibodies, and Chemicals—Full-length mouse Fsp27 was amplified from mouse white adipose tissue cDNA using PCR and inserted into the NdeI/XbaI sites of

* This work was supported by the National Natural Science Foundation of China (Grants 30530350 and 30925017 to P. L.), the Ministry of Education of China (Grant 704002 to P. L.), and the National Basic Research program of China (Grants 2006CB503909 and 2007CB914404) from the Ministry of Science and Technology of China. This work was also supported by the Program for Changjiang Scholars and the Innovative Research Team in University from the Ministry of Education in China.

[S] The on-line version of this article (available at http://www.jbc.org) contains supplemental Figs. S1–S5.

[1] These authors contributed equally to this work.

[2] To whom correspondence should be addressed. Tel./Fax: 86-10-6279-7121; E-mail: li-peng@mail.tsinghua.edu.cn.

[3] The abbreviations used are: Fsp27, fat-specific protein 27; DGAT1, -2, diacylglycerol acyltransferases 1 and 2; LD, lipid droplet; TAG, triacylglycerol; Iso, isoproterenol; HA, hemagglutinin; GFP, green fluorescent protein; aa, amino acid(s); CHX, cycloheximide; OA, oleic acid; siRNA, small interference RNA; HBSS, Hanks' balanced salt solution; CMV, cytomegalovirus; ANOVA, analysis of variance; 2-BrO, 2-bromo-octanoic acid; Fsp3K-A, Fsp27 with mutations in lysine residues 224, 226, and 236; E2, ubiquitin carrier protein; E3, ubiquitin-protein isopeptide ligase; ADRP, adipose differentiation-related protein.

the pCMV5-HA or pCMV5-FLAG vector. Truncated Fsp27 protein and Fsp27 containing amino acid substitution were created using PCR with primers corresponding to the relevant sequences and subcloned into the same restriction sites. The integrity of all plasmid DNA was verified by DNA sequencing.

Antibodies against HA, GFP, tubulin, and ubiquitin were purchased from Santa Cruz Biotechnology (Santa Cruz, CA). Antibodies against FLAG, calnexin, and β-actin were purchased from Sigma. The antibody against COXIV was purchased from Molecular Probes, the antibody against peroxisome proliferator-activated receptor δ was from Abcam (UK), and the antibodies against perilipin A and ADRP (adipose differentiation-related protein) were from Fitzgerald Industries. A rabbit polyclonal antibody against mouse Fsp27 was raised against Fsp27 aa 1–190 (12). Cycloheximide (CHX), MG132, epoxomicin, phenylmethylsulfonyl fluoride, leupeptin, β-glycerol phosphate, isoproterenol, 2-bromo-octanoic acid (2-BrO), sodium orthovanadate, and sodium pyrophosphate were all purchased from Sigma.

Cell Culture and Transfection—HEK293T and 3T3-L1 cells were maintained in Dulbecco's modified Eagle's medium (Invitrogen) containing 10% fetal bovine serum (Invitrogen). The differentiation of the 3T3-L1 cells was initiated 2 days post-confluence by the addition of 5 μg/ml insulin, 1 μM dexamethasone, and 0.5 mM isobutylmethylxanthine (Sigma) and allowed to proceed for 2 days. The differentiation medium was subsequently replaced with Dulbecco's modified Eagle's medium/fetal bovine serum supplemented with only 5 μg/ml insulin for 2 more days before replacing it with normal culture medium. Oleic acids (OAs) were mixed with fatty acid-free bovine serum albumin in water at a 6:1 molar ratio and added directly into the culture medium.

293T cells were transfected using the previously described calcium phosphate co-precipitation technique (14) or Lipofectamine 2000 (Invitrogen) according to the manufacturer's instruction. 3T3-L1 adipocytes were transfected with plasmid DNA by electroporation. Briefly, on day 7 after differentiation induction, adipocytes were detached from culture dishes with 0.25% trypsin and 1 mg/ml EDTA in phosphate-buffered saline, washed twice, and resuspended in buffer L (Amaxa, Germany).

Approximately 2×10^6 cells were then mixed with 1 μg of plasmid DNA encoding GFP-CB5, which was delivered to the cells by a pulse of electroporation with an Amaxa Nucleofector (Amaxa). After electroporation, cells were immediately mixed with fresh medium and reseeded onto coverslips for the immunofluorescence staining.

Fsp27 Stability Assay—Fsp27 stability in 293T cells or 3T3-L1 adipocytes was measured using a CHX-based protein-chase experiment. For 293T cells, an expression plasmid encoding HA-tagged Fsp27, its truncation, or its mutant was transfected using the calcium phosphate method. Twenty-four hours post-transfection, the medium was replaced with fresh Dulbecco's modified Eagle's medium plus 10% fetal bovine serum, followed by the addition of CHX (100 μg/ml). Cells were harvested at different time points after the addition of CHX. To determine the stability of endogenous Fsp27 in 3T3-L1 adipocytes, on day 8 after induction cells were treated with CHX and harvested in the same manner as the 293T cells. For quantitative analysis, the Western blot bands were further quantified with Quantity One software (Bio-Rad).

Ubiquitin Conjugation Assay—293T cells were transfected with FLAG-Fsp27 or FLAG-Fsp3K-A using the calcium phosphate co-precipitation technique. Twenty-four hours post-transfection, the cells were treated with 10 μM MG132 for 2 h or left untreated. The cells were then harvested, sonicated in lysis buffer (20 mM Tris-HCl, pH 7.4, 150 mM NaCl, 1 mM EDTA, 1 mM EGTA, 1% Trion X-100, 2.5 mM sodium pyrophosphate, 1 mM β-glycerol phosphate, 1 mM sodium orthovanadate, 2 μg/ml leupeptin, and 1 mM phenylmethylsulfonyl fluoride) with the addition of 1% SDS, and heated at 90 °C for 5 min. The heated lysates were then cooled and centrifuged at 13,000 × *g* for 30 min. The supernatant was removed and diluted with lysis buffer until the concentration of SDS reached 0.1%. The diluted samples were used for immunoprecipitation with M_2 beads conjugated with a FLAG-specific antibody (Sigma). Immunoprecipitates or total cell lysates were subjected to SDS-PAGE and Western blot analysis. In experiments based on 3T3-L1 adipocytes, endogenous Fsp27 was immunoprecipitated using an antibody against Fsp27.

Virus Preparation and Generation of Stable Cell Lines—A DNA fragment encoding an siRNA specific for Fsp27 (5′-CTGTCTAGACAAAAAGGTCCAGGACATCTTGAAATCTCTTGAATTTCAAGATGTCCTGGACCGGGGATCTGTGGTCTCATACA-3′) was inserted into the FG12 expression vector (gift from Dr. Zilong Wen, Hong Kong University of Science and Technology) and packaged into a lentivirus as described previously (15). Culture medium containing virus particles was filtered through a 0.22-μm filter and centrifuged at 50,000 × *g* for 20 min to concentrate the virus particles. The virus pellet was resuspended in HBSS (Invitrogen), layered on top of a sucrose cushion (20% sucrose in HBSS), and centrifuged at 50,000 × *g* for 20 min. Finally, the virus pellet was resuspended in HBSS and frozen in −80 °C until further use. 3T3-L1 preadipocytes were infected for 12 h with the lentivirus expressing the Fsp27-specific siRNA. After several passages, infected preadipocytes that stably expressed the siRNA were used as an Fsp27 knockdown cell line, and differentiation was induced. Because all lentiviruses contain a GFP expression unit, GFP was used as a control for viral infection efficiency. A lentivirus generated from the empty vector, which expressed only GFP, was used as a negative control. Recombinant adenoviruses encoding the CMV promoter-driven, HA-tagged Fsp27, HA-tagged Fsp3K-A, or GFP were constructed using the AdEasy-1 system (Stratagene).

RNA Interference, RNA Extraction, and Quantitative Real-time PCR Analysis—siRNAs against DGAT1 and DGAT2 were chemically synthesized (Invitrogen) and transfected into 3T3-L1 adipocytes using Lipofectamine 2000 on day 5 after induction of differentiation. The sequences of the sense siRNAs were DGAT1, 5′-GAUUCUUUGUUCAGCUCAGACTT-3′ and DGAT2, 5′-GACAUCUUCUCUGUCACCUGGTT-3′ (16). Forty-eight hours after siRNA transfection, total RNA was isolated using the TRIzol reagent (Invitrogen). First-strand cDNAs were synthesized from 5 μg of total RNA using oligo-$(dT)_{20}$ primers and the Superscript III RT kit (Invitrogen) according to the manufacturer's instructions. Real-time PCR was performed using the ABI SYBR Green PCR Master Mix in a

MX3000P real-time PCR system (Stratagene) according to the manufacturer's instruction. The result was normalized to the β-actin level in each sample. The primer sequences for real-time PCR analysis were: ActinF, 5′-ACACTGTGCCCATCTACGAG-3′; ActinR, 5′-CAGCACTGTGTTGGCATAGAG-3′; Fsp27F, 5′-TCGTGTTAGCACCGCAGAT-3′; Fsp27R, 5′-GCTCTCTTCTTGCGCTGTT-3′; DGAT1F, 5′-TCCGTCCAGGGTGGTAGTG-3′; DGAT1R, 5′-TGAACAAAGAATCTTGCAGACGA-3′; DGAT2F, 5′-CTGGCTGATAGCTGCTCTCTACTTC-3′; and DGAT2R, 5′-TGTGATCTCCTGCCACCTTTC-3′.

Subcellular Fractionation—To determine the precise subcellular localization of endogenous Fsp27 in adipocytes, differentiated 3T3-L1 cells were harvested in buffer (0.5 M sucrose, 5 mM $MgCl_2$, and 37.5 mM Tris maleate, pH 6.4) and homogenized using a Polytron homogenizer (Kinematica); the resulting homogenate was centrifuged at 300 × *g* for 1 min. The upper fat cake was removed, and the transparent fluid between the fat and the pellet was centrifuged again at 5,000 × *g* for 15 min. The pellet was resuspended in buffer (0.25 M sucrose, 5 mM $MgCl_2$, and 10 mM Tris-HCl, pH 7.4), after which it was filtered through two layers of gauze and layered on top of a 2.2 M sucrose cushion and centrifuged at 80,000 × *g* for 80 min. The resulting pellet was resuspended in Laemmli buffer as the nuclear fraction. The supernatant remaining after the 5,000 × *g* centrifugation step was centrifuged again at 8,500 × *g* for 30 min. The resulting supernatant was layered on top of a discontinuous sucrose gradient consisting of 2.0 M, 1.5 M, and 1.3 M sucrose and centrifuged at 100,000 × *g* for 120 min. The interphase between the 1.3 M and 1.5 M layers and the 1.5 M and the 2.0 M layers was collected as the microsome fraction. The remaining supernatant was centrifuged again and collected as the cytosolic fraction. The pellet from the 8,500 × *g* centrifugation step was resuspended in buffer (25 mM mannitol, 5 mM HEPES, pH 7.4, 0.5 mM EGTA, and 0.1% bovine serum albumin), layered on a 30% Percoll gradient, and centrifuged at 95,000 × *g* for 30 min. Mitochondria were recovered from a band formed one-third distance from the bottom and washed with buffer (250 mM mannitol, 5 mM HEPES, and 0.5 mM EGTA).

The subcellular fractionation for comparing the Fsp27 protein level in the LD and ER fractions from untreated cells or cells treated with Iso was essentially the same as described previously (17) with minor modifications. 3T3-L1 adipocytes were resuspended in TES buffer (20 mM Tris-HCl, 1 mM EDTA, 8.7% sucrose, pH 7.4) and disrupted using a loose-fitting Dounce homogenizer (30 strokes); they were then directly subjected to centrifugation at 8,000 × *g* for 15 min. To isolate the LD fraction, the upper fat cake was removed from the centrifuge tube and diluted to a final volume of 8.5 ml with TES buffer. 2 ml of hypotonic buffer (10 mM Tris-HCl, pH 7.4, 1 mM EDTA, 1 mM phenylmethylsulfonyl fluoride) was loaded on top of it. After centrifugation at 50,000 × *g* for 30 min, the upper fat cake was harvested and washed several times with hypotonic buffer. Half of the sample was used for Western blot as the LD fraction, and the other half was used for lipid extraction.

Immunofluorescence Staining—A primary antibody against Fsp27 was added at a 1:300 dilution and incubated with the samples for 2 h at room temperature. An Alexa Fluor 568-conjugated goat anti-rabbit IgG antibody (Molecular Probes) was used as the secondary antibody. For visualization of neutral lipids, BODIPY 493/503 (Molecular Probes) was used. Sections were observed using a Zeiss 200M inverted microscope, and images were captured with an AxioCam MRm camera and AxioVision software 4.5 (Zeiss).

Measurement of TAG Content—The method for measuring TAG content of 3T3-L1 adipocytes was essentially the same as described previously (12). For quantitative analysis, the TAG spots of the samples and TAG standard on the TLC plates (Sigma) were scanned and quantified using Quantity One software (Bio-Rad). Then numerical values of TAG standard spots given by Quantity One were used to make a standard curve according to the linear regression equation. The TAG contents of samples were calculated by the standard curve. For relative TAG levels, the value of control group was denoted as 1.

Statistical Analysis—Significant difference between the stability curves was evaluated using two-way ANOVA (Prism 4.00, GraphPad). To statistically analyze the significant difference between two parameters, a two-tailed Student's *t* test (unpaired) was used. The results are presented as the mean ± S.D.

RESULTS

Fsp27 Is Unstable and Ubiquitinated in Adipocytes—To determine whether protein stability plays a role in regulating the steady-state level of the Fsp27 protein in differentiated 3T3-L1 adipocytes, we measured the level of Fsp27 protein in the presence of CHX, which blocks protein synthesis. Fsp27 was very unstable (Fig. 1*A*), with a half-life of ~15 min (Fig. 1*B*). To further evaluate which pathway regulates Fsp27 stability, we measured the rate of Fsp27 degradation in differentiated 3T3-L1 adipocytes in the presence of various protease inhibitors. As shown in Fig. 1*C*, in the presence of the general protease inhibitor leupeptin or the lysosomal inhibitor ammonium chloride (NH_4Cl), a smaller amount of Fsp27 accumulated in cells treated with CHX. By contrast, when cells were treated with CHX in the presence of the proteasome-specific inhibitors MG132 or epoxomicin, a larger amount of Fsp27 accumulated, indicating that degradation of Fsp27 is controlled by the proteasome-dependent degradation pathway.

Next, an *in vivo* ubiquitination assay was performed to assess whether Fsp27 is ubiquitinated prior to degradation. Differentiated 3T3-L1 adipocytes were treated with MG132 and incubated for an additional 2 h. Fsp27 was then immunoprecipitated with an anti-Fsp27 antibody. As shown in Fig. 1*D*, when blotted with an anti-ubiquitin antibody, a typical protein ladder of higher molecular weight species was observed, suggesting that Fsp27 was polyubiquitinated. By contrast, no ubiquitin signal was detected in the immunoprecipitated products from adipocytes in the absence of MG132 or from 3T3-L1 preadipocytes that do not express Fsp27. Our data indicate that the Fsp27 protein level can be controlled via the ubiquitin-dependent proteasomal degradation pathway.

The C-terminal Region of Fsp27 Is Important for Controlling Its Stability—To identify the region of Fsp27 that mediates its degradation, we generated HA-tagged wild-type and truncated Fsp27, overexpressed them in 293T cells, and measured their rate of degradation. Consistent with the data in differentiated

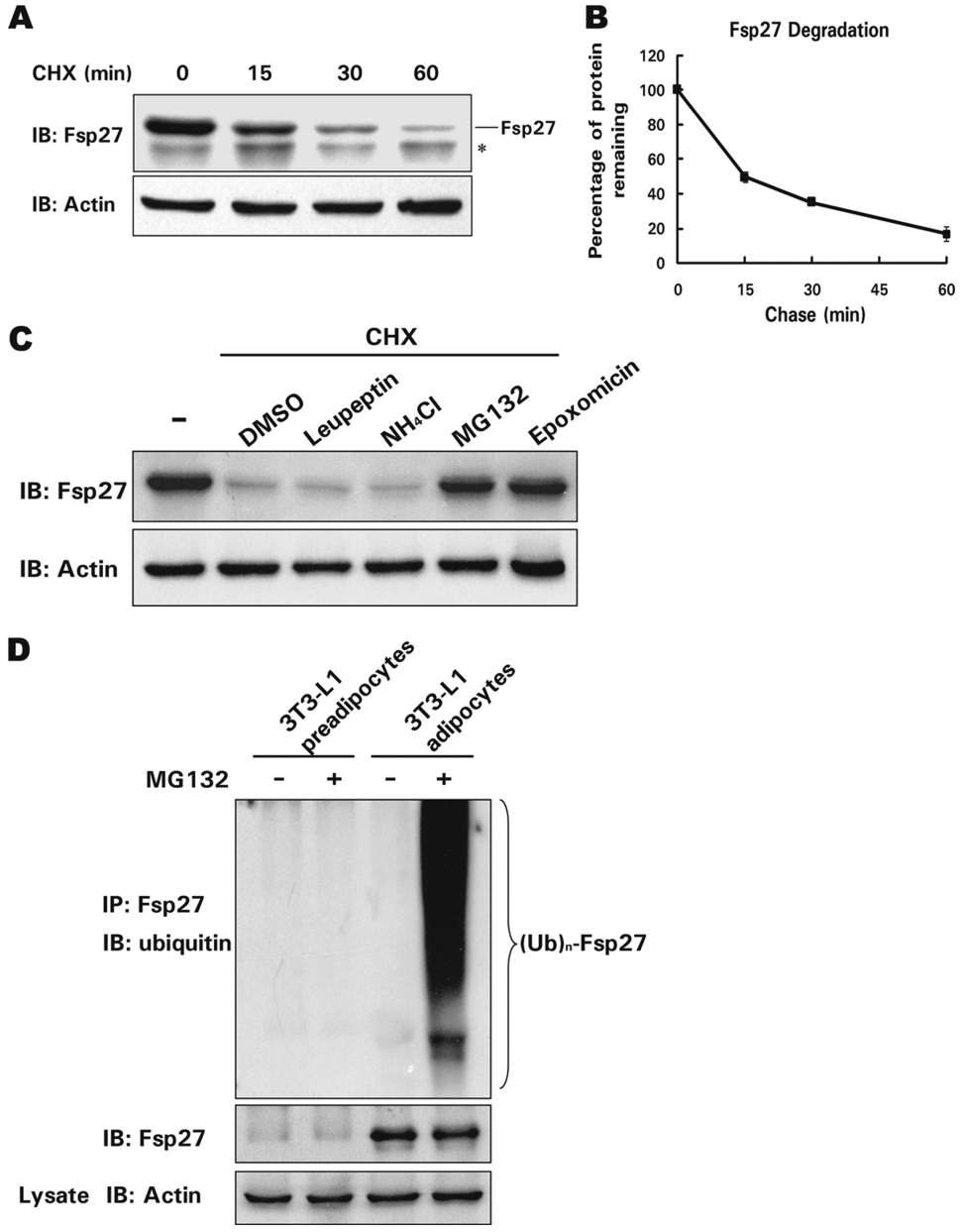

FIGURE 1. **Fsp27 is a short lived protein, and its degradation is dependent on proteasome activity in adipocytes.** *A*, Fsp27 is a short lived protein in adipocytes. Fsp27 stability was evaluated in a cycloheximide (*CHX*, 100 μg/ml) chasing experiment. CHX was added to the culture medium of 3T3-L1 adipocytes that had been differentiated for 8 days. Cells were harvested 0, 15, 30, or 60 min after the addition of CHX. The Fsp27 protein level was evaluated using Western blot with an antibody against Fsp27. *IB*, immunoblot. The *asterisk* designates a nonspecific band recognized by the Fsp27 antibody. β-Actin was used as a loading control. *B*, quantitative analysis of the Fsp27 level in *A* using Quantity One software. The Fsp27 level before CHX treatment was designated as 100%. Experiments were repeated three times. *C*, Fsp27 degradation is dependent on proteasome activity. Differentiated 3T3-L1 adipocytes were pretreated with DMSO, 5 μg/ml leupeptin (an inhibitor of trypsin and cysteine proteases), 10 μM NH_4Cl (a general lysosomal protease inhibitor), or 10 μM MG132 or 1 μM epoxomicin (both proteasome-specific inhibitors) for 30 min. CHX was then added to the culture medium for 45 min, and the Fsp27 protein level was evaluated using Western blotting. *D*, Fsp27 is polyubiquitinated. Fsp27 from differentiated 3T3-L1 adipocytes treated with or without MG132 (10 μM) for 2 h was immunoprecipitated with an antibody against Fsp27. The level of Fsp27 ubiquitination was detected using an antibody against ubiquitin. Untreated 3T3-L1 preadipocytes or preadipocytes treated with MG132 were used as negative controls for Fsp27 expression and ubiquitination. *IP*, immunoprecipitation. *$(Ub)_n$-Fsp27* denotes polyubiquitinated Fsp27.

adipocytes, Fsp27 was unstable, with a half-life of ~30 min. Interestingly, truncated Fsp27 containing the N-terminal region (aa 1–191) was much more stable, with a half-life of >2 h compared with the 30 min for wild-type Fsp27. By contrast, truncated Fsp27 containing the C-terminal (aa 172–239) domain had a half-life similar to that of wild-type Fsp27, indicating that the C-terminal region contains the signals that render Fsp27 unstable (Fig. 2, *A* and *B*). Furthermore, the degradation rate of wild-type Fsp27 was reduced in the presence of MG132, and more Fsp27 protein accumulated. Additionally, the rapid degradation of truncated Fsp27 (aa 172–239) was also mediated by the ubiquitin-dependent proteasomal degradation pathway, because its degradation could be blocked by MG132 (Fig. 2*C*).

Fsp27 Stability Is Regulated by Three Lysine Residues in the C-terminal Region—Crucial lysine residues of proteins degraded through the ubiquitin-dependent proteasomal degradation pathway serve as predominant acceptor sites for covalent ubiquitin attachment. To identify the lysine(s) that regulate(s) Fsp27 stability, we first aligned the Fsp27 C-terminal sequences (aa 191–239) of different species and identified three conserved lysine residues within this region (Lys-224, Lys-226, and Lys-236 (Fig. 2*D*)). We then carried out site-directed mutagenesis to substitute these lysine residues with alanine individually or in combination. HA-tagged Fsp27 mutants in which lysines 224 and 226 were substituted with alanines (K224/226–2A) or in which lysine 236 was substituted with alanine (K236A) had a degradation rate similar to that of the wild-type protein. However, HA-tagged Fsp27 with mutations in all three lysine residues (Fsp3K-A) had a dramatically increased stability, with a half-life of ~2 h compared with that of 30 min for the wild-type protein (Fig. 2, *E* and *F*). Consistent with its increased stability, FLAG-tagged Fsp3K-A was less ubiquitinated compared with wild-type protein (Fig. 2*G*, *lane 3* and *4*). These data suggest that the three lysines in the C-terminal region play a central role in Fsp27 stability, probably by functioning as acceptor sites for ubiquitin ligation.

Overexpression of Mutant Fsp27 Defective in Ubiquitination Enhances Endogenous Fsp27 Stability and Increases Lipid Storage in Adipocytes—To assess the physiological relevance of Fsp27 stability in differentiated adipocytes, we generated an adenovirus that expresses HA-tagged Fsp3K-A and used it to infect differentiated

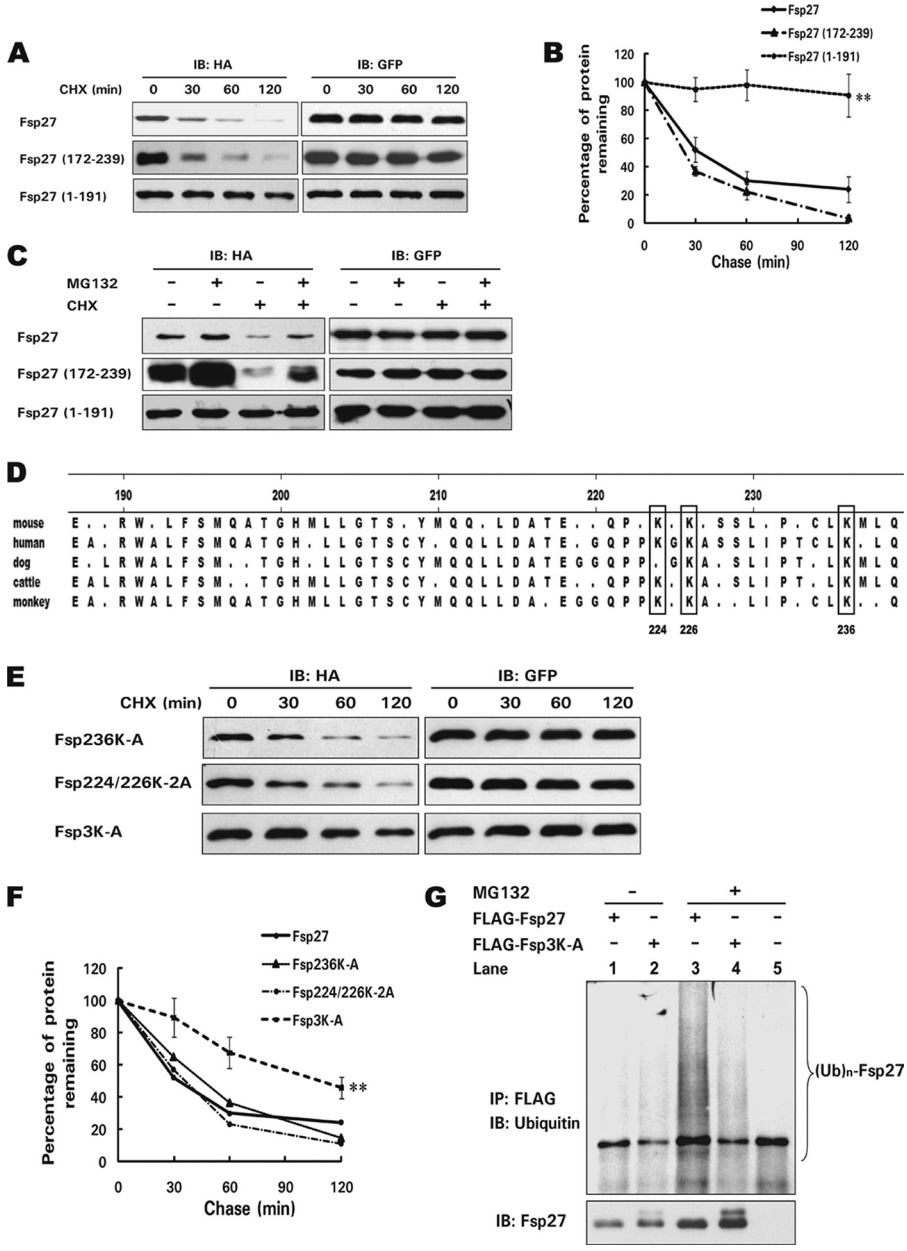

FIGURE 2. **Three lysine residues in the C-terminal region of Fsp27 are essential for its ubiquitination and degradation.** *A*, the C-terminal region (aa 172–239) of Fsp27 has a short half-life. 293T cells were transfected with 0.5 μg of HA-tagged wild-type Fsp27 or various truncations (aa 1–191 and 172–239) for 24 h. Cells were harvested 0, 30, 60, or 120 min after the addition of CHX, and the protein level was analyzed using Western blotting. A GFP-expressing plasmid was co-transfected with the Fsp27 expression plasmid, and GFP was used as a transfection and loading control. *B*, quantitative analysis of the relative level of Fsp27 and its truncations based on the results in *A*. Experiments were repeated three times. **, significant difference from wild-type Fsp27 degradation curve using a two-way ANOVA, $p < 0.01$. *C*, the degradation of HA-tagged wild-type or truncated Fsp27 (aa 172–239) in 293T cells is dependent on proteasome activity. The MG132 treatment is similar to that described in Fig. 1*C*. *D*, amino acid sequence alignment of the C-terminal region of Fsp27 from various species. Consensus amino acids were determined using the ClustalV method, and the *three boxes* indicate conserved lysine residues at positions 224, 226, and 236. *E*, increased stability of Fsp27 with mutations in all three lysine residues (Fsp3K-A) in 293T cells. 0.5 μg of HA-tagged Fsp236K-A (lysine residue at 236 was substituted with alanine), Fsp224/226K-2A (lysine residues at 224 and 226 were replaced with alanines), or Fsp3K-A (lysine residues at 224, 226, and 236 were substituted with alanines) was transfected into 293T cells, and their degradation was assayed using the CHX chasing experiment. *F*, quantitative analysis of the relative level of Fsp27 mutants from *E*, which shows a longer half-life of Fsp3K-A. Experiments were repeated three times. **, significant difference from wild-type Fsp27 degradation curve using a two-way ANOVA, $p < 0.01$. *G*, decreased polyubiquitination level of Fsp3K-A. 293T cells were transfected with 0.5 μg of FLAG-tagged wild-type Fsp27 or Fsp3K-A. MG132 was added for 2 h to enhance the accumulation of polyubiquitinated proteins. In the presence of MG132, the polyubiquitinated protein level of Fsp3K-A was lower than that of wild-type Fsp27 (*lanes 3* and *4*). The pCMV5-FLAG empty vector was used as a negative control (*lane 5*). *$(Ub)_n$-Fsp27* denotes polyubiquitinated Fsp27 or Fsp3K-A.

3T3-L1 adipocytes. As expected, the stability of Fsp3K-A was higher than that of endogenous Fsp27 (Fig. 3*A*). Interestingly, we also observed significantly increased stability for endogenous Fsp27 when Fsp3K-A was overexpressed (Fig. 3, *A* and *B*). The increased stability of wild-type Fsp27 was also observed when co-expressed with Fsp3K-A in 293T cells (data not shown).

To further determine the functional correlation of the increased stability of Fsp3K-A and eliminate the effect of endogenous Fsp27, we generated Fsp27 knockdown cells by infecting 3T3-L1 preadipocytes with a lentivirus encoding a siRNA specific for Fsp27. After a few generations of selection, we obtained 3T3-L1 adipocytes in which Fsp27 expression was dramatically reduced after differentiation (90% lower than in cells that were infected with a lentivirus expressing only GFP) (Fig. 3*C*). We then infected the Fsp27-depleted adipocytes with the adenovirus encoding HA-tagged Fsp27 or Fsp3K-A and observed a higher level of Fsp3K-A compared with that of wild-type Fsp27 (Fig. 3*C*). Furthermore, the stability of Fsp3K-A was increased compared with that of wild-type Fsp27 (Fig. 3*D*).

Next, we evaluated the functional consequence of ectopically expressed Fsp3K-A on the TAG content of adipocytes. The cellular TAG content of Fsp27-deficient adipocytes was significantly decreased compared with wild-type adipocytes (Fig. 3*E*). The overexpression of Fsp27 mediated by adenovirus infection restored the cytosolic lipid content to a level similar to that of differentiated wild-type 3T3-L1 cells. More relevant was the observation that the overexpression of Fsp3K-A increased lipid storage to a much higher level than the overexpression of wild-type Fsp27 (~30% higher, $p < 0.05$, Fig. 3*E*). These data suggest that mutant Fsp27 with its improved stability could enhance endogenous Fsp27 stability and increase lipid storage in differentiated 3T3-L1 adipocytes.

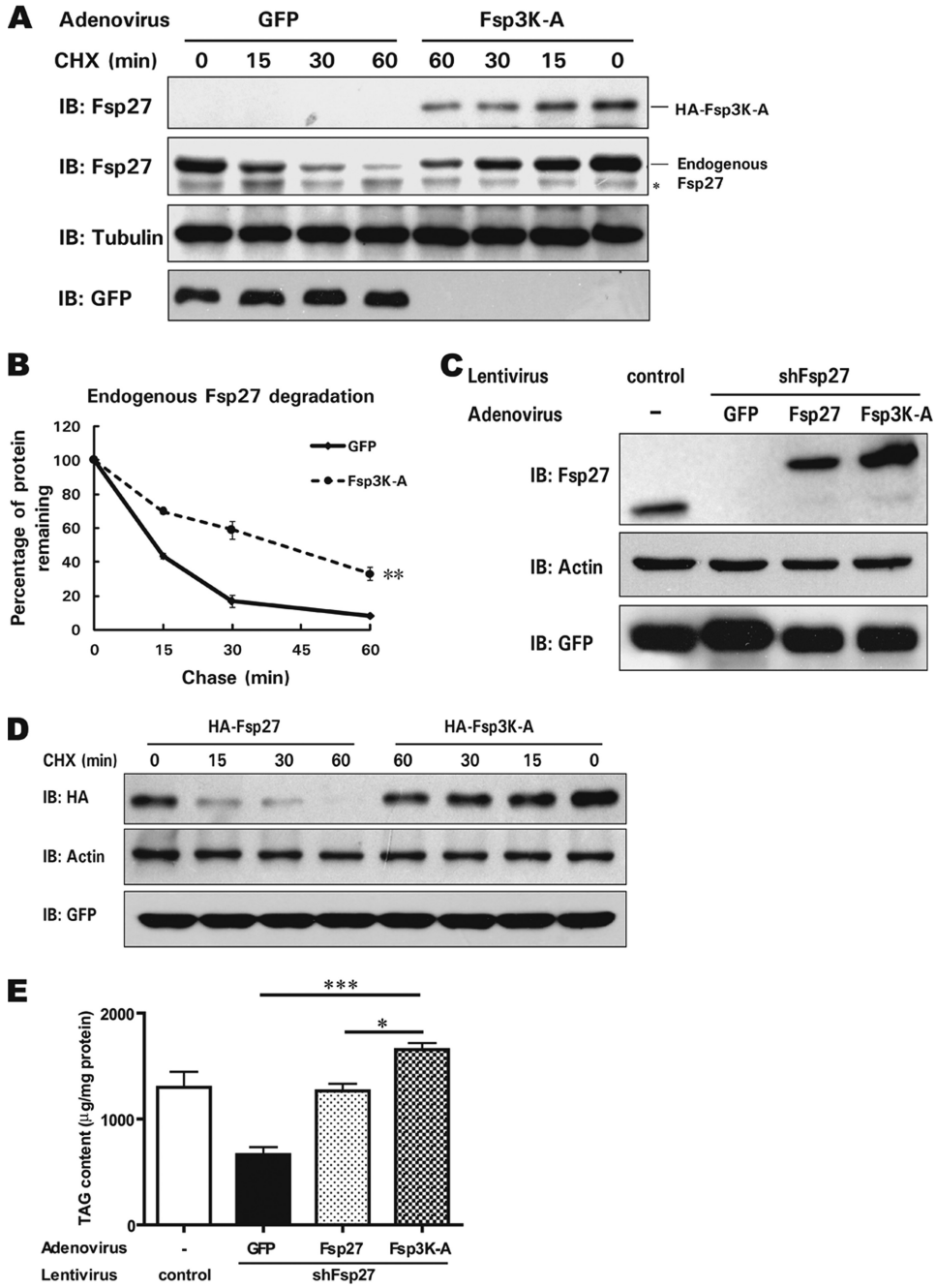

FIGURE 3. **Fsp3K-A enhances endogenous Fsp27 stability and promotes lipid storage in adipocytes.** *A*, the expression of Fsp3K-A in differentiated 3T3-L1 adipocytes enhances the stability of endogenous Fsp27. Differentiated 3T3-L1 cells (day 6 after induction) were infected with an adenovirus encoding HA-tagged Fsp3K-A or GFP as a negative control. Two days after infection, cells were harvested 0, 15, 30, or 60 min after the addition of CHX. *B*, the quantitative analysis of the level of endogenous Fsp27 from *A*. Experiments were repeated three times. **, significant difference from control curve using a two-way ANOVA, $p < 0.01$. *C*, knockdown of Fsp27 in 3T3-L1 adipocytes using lentivirus-delivered siRNA against Fsp27 and overexpression of HA-Fsp27, HA-Fsp3K-A, or GFP in Fsp27-deficient 3T3-L1 adipocytes mediated by adenovirus infection. A lentivirus generated from the empty vector, which encoding only GFP, was used as a negative control. *D*, increased Fsp3K-A stability in Fsp27-deficient 3T3-L1 adipocytes. Differentiated Fsp27-deficient 3T3-L1 adipocytes were infected with an adenovirus encoding HA-tagged wild-type Fsp27 or Fsp3K-A. Two days after infection, cells were harvested at the indicated time points after the addition of CHX for stability analysis. *E*, Fsp3K-A promotes lipid storage in adipocytes. Fsp27-deficient 3T3-L1 adipocytes were infected with an adenovirus encoding HA-Fsp27, HA-Fsp3K-A, or GFP for 2 days, and the total cellular lipids were extracted. The cellular TAG content was evaluated using TLC. A Student's two-tailed *t* test (unpaired) was used for statistical analysis (*, $p < 0.05$; ***, $p < 0.001$, $n = 3$).

Fsp27 Is Stabilized by β-Agonist Isoproterenol Treatment—Because Fsp27 is an important metabolic regulator in adipocytes, we examined whether factors that influence lipid metabolism in adipocytes, including fatty acids, insulin, and β-agonists, could regulate its protein level. The addition of bovine serum albumin-complexed OAs to the culture medium of differentiated 3T3-L1 cells led to a gradual increase in the Fsp27 level (Fig. 4*A*). This increase was not due to increased Fsp27 transcription as the mRNA level remained consistent during the course of OA treatment (supplemental Fig. S1). The short term treatment of differentiated adipocytes with insulin (2 h) did not alter the Fsp27 protein level or its stability (data not shown). Surprisingly, isoproterenol, a β-agonist that activates the β-adrenergic pathway and stimulates lipolysis in 3T3-L1 adipocytes, significantly increased the Fsp27 protein level within half an hour of treatment. The Fsp27 protein level was three times higher after 3 h of Iso treatment (Fig. 4*B* and supplemental Fig. S2). An increased Fsp27 level was also observed in 3T3-L1 adipocytes that were treated with forskolin, an activator of adenylyl cyclase that leads to the activation of protein kinase A and downstream lipolysis (data not shown). However, the level of perilipin A, another LD-associated protein in adipocytes, was similar in the presence or absence of Iso, while phosphorylation of perilipin A was observed when cells were treated with Iso (Fig. 4*B*). The increase in the Fsp27 protein level in the presence of Iso was not due to increased Fsp27 transcription, because the Fsp27 mRNA level was similar throughout the course of Iso treatment (supplemental Fig. S3).

We next examined whether the Iso-induced rapid increase in the Fsp27 level is due to enhanced protein stability. Indeed, we observed markedly increased Fsp27 stability in Iso-treated cells, with a half-life of ~1 h compared with that of 15 min in untreated cells (Fig. 4, *C* and *D*). Consistent with the enhanced stability, the level of Fsp27 ubiquitination was reduced in the presence of Iso (Fig. 4*E*). Kinetic analysis of the Fsp27 protein level after Iso withdrawal demonstrated that the level of Fsp27 remained high for ~4 h and then gradually declined to a normal level 12 h after

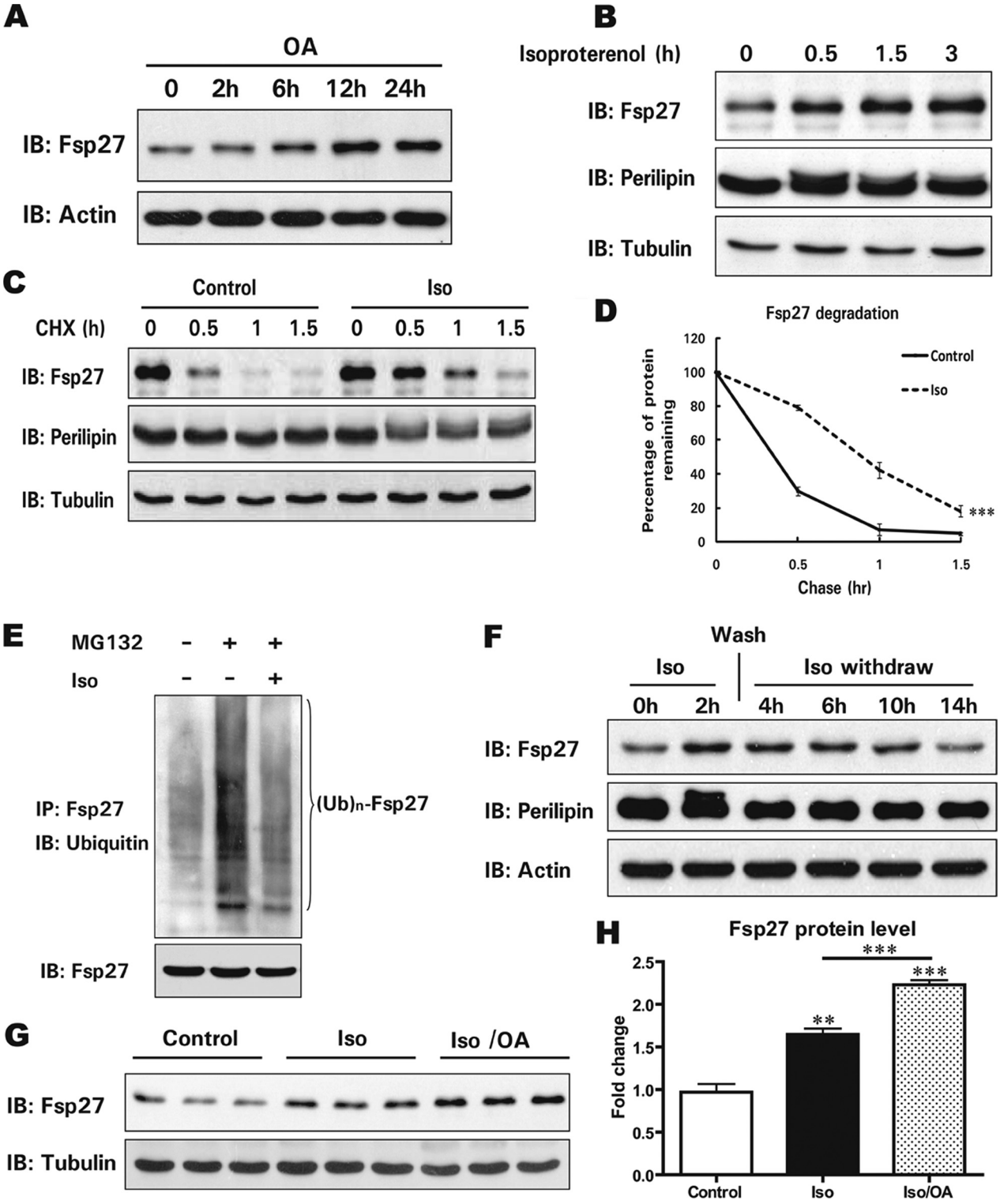

FIGURE 4. **A β-agonist stimulates Fsp27 accumulation and increases Fsp27 stability.** *A*, oleic acids (*OA*) promote Fsp27 accumulation. Differentiated 3T3-L1 adipocytes (8 days after induction) were treated with OA (400 μM) for 0, 2, 6, 12, or 24 h, and the Fsp27 protein level was analyzed. β-Actin was used as a loading control. *B*, Iso stimulates Fsp27 accumulation. Differentiated 3T3-L1 adipocytes were treated with Iso (10 μM) for the indicated amount of time (0, 0.5, 1.5, or 3 h), and the Fsp27 level was evaluated. Perilipin A was used as a control for the LD-associated protein. Tubulin was used as a loading control. *C*, Iso enhances Fsp27 stability. Differentiated 3T3-L1 adipocytes were treated with CHX in the presence or absence of Iso. Cells were harvested 0, 30, 60, or 90 min after the addition of Iso and CHX. *D*, the quantitative analysis of the Western blot in *C* demonstrated that Fsp27 had an increased half-life in the presence of Iso. Experiments were repeated three times. ***, significant difference from control curve using a two-way ANOVA, $p < 0.001$. *E*, reduced Fsp27 ubiquitination in 3T3-L1 adipocytes treated with Iso. Differentiated 3T3-L1 adipocytes were treated with MG132 alone or together with Iso for 2 h. Fsp27 was immunoprecipitated, and the ubiquitination level was determined using a ubiquitin-specific antibody. *F*, kinetic analysis of the Fsp27 level after Iso withdrawal in 3T3-L1 adipocytes. Cells were harvested at various time points after Iso treatment and withdrawal. Iso was washed away from the culture medium 2 h after its addition. *G*, OA enhanced Iso-induced Fsp27 accumulation. Differentiated 3T3-L1 adipocytes were treated with Iso alone or together with OA for 1 h, and the Fsp27 protein level was analyzed using Western blot. *H*, quantitative analysis of the Fsp27 level in *G*. A Student's two-tailed *t* test (unpaired) was used for statistical analysis (***, $p < 0.001$; **, $p < 0.01$, $n = 3$).

Iso withdrawal (Fig. 4*F* and supplemental Fig. S4). To further confirm the observation that Iso could induce Fsp27 accumulation, we added Iso to the culture medium alone or in combination with OA. Although the addition of OA alone for the first 2 h did not result in an increased Fsp27 level as shown above (Fig. 4*A*), incubation with OA and Iso led to a further increase in Fsp27 level (2.2-fold) compared with the treatment of Iso alone (1.6-fold) ($p < 0.001$, Fig. 4, *G* and *H*). However, the Iso- or forskolin-induced Fsp27 accumulation was not observed when Fsp27 was ectopically expressed in NIH-3T3 cells (data not shown). These data suggest that Fsp27 was stabilized and maintained at a higher level in 3T3-L1 adipocytes in the presence of β-agonists. Although the direct effect of treatment with a β-agonist most likely occurred through the activation of the protein kinase A pathway, the increased Fsp27 stability was not due to its phosphorylation, as we observed no phosphorylation of Fsp27 in the presence of Iso in 3T3-L1 adipocytes (data not shown).

Accumulation of Fsp27 in Adipocytes Is Dependent on TAG Synthesis—One of the major effects of β-agonist treatment in adipocytes is dramatically enhanced lipolysis due to the phosphorylation of perilipin A by protein kinase A and the translocation of hormone-sensitive lipase to LDs (4, 18, 19). The large amount of free fatty acids released during lipolysis can be re-esterified to generate TAGs that are incorporated into nascent LDs. Because Fsp27 is stabilized in a process initiated by a β-agonist, we tested the effect of TAG synthesis on Fsp27 accumulation by the addition of 2-BrO, which has been shown to inhibit the activity of DGAT and block the last step of TAG synthesis (20, 21). Although the Fsp27 level was increased in the presence of Iso, the level was decreased in the presence of 2-BrO (50% reduction, $p < 0.01$). Intriguingly, Iso treatment in the presence of 2-BrO exacerbated the decrease in the Fsp27 level (80% reduction, $p < 0.001$, Fig. 5, *A* and *B*). To further confirm that Fsp27 protein stability was dependent on TAG synthesis and fatty acid esterification, we depleted DGAT1 and DGAT2 individually or in combination in 3T3-L1 adipocytes by transfecting specific siRNAs against DGAT1 and DGAT2. The individual siRNA knockdown efficiency was evaluated by quantitative real-time PCR analysis and was shown to be ~50% for each isozyme (Fig. 5, *C* and *D*). The efficiency of knocking down DGAT1 and DGAT2 in combination was ~35% for DGAT1 and 30% for DGAT2 (Fig. 5*E*). As expected, the TAG level was reduced ~40–50% following the silencing of DGAT1 and DGAT2 individually or in combination (Fig. 5*F*). More importantly, the Fsp27 protein level was decreased significantly when the DGAT expression was reduced (Fig. 5, *G* and *H*). The decreased Fsp27 level in DGAT knockdown cells is likely due to reduced Fsp27 stability as the Fsp27 mRNA level in DGAT knockdown cells was similar to that of control cells transfected with a scrambled siRNA (data not shown). These data strongly suggest that the Fsp27 protein level was regulated by DGAT activity, TAG synthesis, and LD formation. Therefore, Fsp27 is stabilized in a TAG synthesis-dependent cellular process, which could be enhanced by providing extra fatty acids as the substrate for TAG synthesis.

Increased Lipid Droplet Association of Fsp27 after Isoproterenol Treatment—Although Fsp27 was found to be a LD-associated protein, its precise subcellular localization in adipocytes has not been determined. Using a biochemical fractionation approach, we isolated various subcellular organelles from 3T3-L1 adipocytes and examined the Fsp27 level. By loading the same percentage of each fraction onto a SDS-polyacrylamide gel, we observed that the majority of Fsp27 was localized to the ER-enriched microsomal fraction, and that Fsp27 was absent from the mitochondrial fraction. A small amount of Fsp27 was detected in the cytosolic and nuclear fractions. The purity of each fraction was evaluated using organelle-specific markers. Tubulin, a cytosolic protein, was only detected in the cytosolic fraction. COXIV, a mitochondrial-specific protein, was detected at a high level in the mitochondria. Calnexin and peroxisome proliferator-activated receptor δ were used as specific markers for the ER and nucleus, respectively (22) (Fig. 6*A*). These data suggest that, in addition to being localized to LDs as previously demonstrated, Fsp27 is also localized to the ER, where Cidea and Cideb are localized (7, 12, 23, 24). To further confirm the ER localization of Fsp27, immunofluorescence was performed on 3T3-L1 adipocytes. Endogenous Fsp27 protein was stained with a rabbit anti-Fsp27 antibody, whereas the ectopically expressed ER marker GFP-CB5 was used to visualize the ER network. In addition to localizing to LDs, a large amount of Fsp27 co-localized with the ER-specific protein CB5 (Fig. 6*B*). These data strongly suggest that Fsp27 is also localized to the ER.

Next, we tested whether the increase in the Fsp27 level was coupled to the increased localization to the ER and LDs during β-agonist stimulation. We isolated the ER and LD fractions from untreated 3T3-L1 adipocytes or those treated with Iso for 2 h. Tubulin and calnexin were used as specific markers for the cytosolic and ER fractions, respectively. ADRP was detected in the LD fraction (Fig. 6*C*). The amount of Fsp27 associated with LDs following Iso treatment significantly increased when a similar percentage of each fraction was loaded (more than 3-fold higher, Fig. 6*C*, *lanes 8* and *4*). When sample loading was normalized to the TAG level in the LD fractions, the Fsp27 level on the LDs was also greatly increased after Iso treatment (more than 4-fold higher, Fig. 6*D* and supplemental Fig. S5*A*). An increased amount of ADRP on the LDs was also observed in cells treated with Iso (Fig. 6*D*). We then normalized the sample loading to the amount of the LD-associated protein ADRP and also observed a higher level of Fsp27 in the LD fraction following Iso treatment (Fig. 6*E*). Additionally, the amount of Fsp27 on the ER was slightly increased in Iso-treated cells (<50% higher, Fig. 6*F* and supplemental Fig. S5*B*); however, this increase was much lower than the increase observed on the LDs. Morphologically, after treatment with Iso for 2 h, 3T3-L1 adipocytes had more small and dispersed LDs. Moreover, there was a notable increase in the staining signal of Fsp27 on the LDs, which further confirms the Fsp27 accumulation on LDs during Iso treatment (Fig. 6*G*). These data suggest that increased Fsp27 during Iso treatment preferentially associated with LDs.

DISCUSSION

We have demonstrated here that Fsp27, a protein localized to the ER and LDs, has a short half-life and undergoes ubiquitin-dependent proteasomal degradation that is dy-

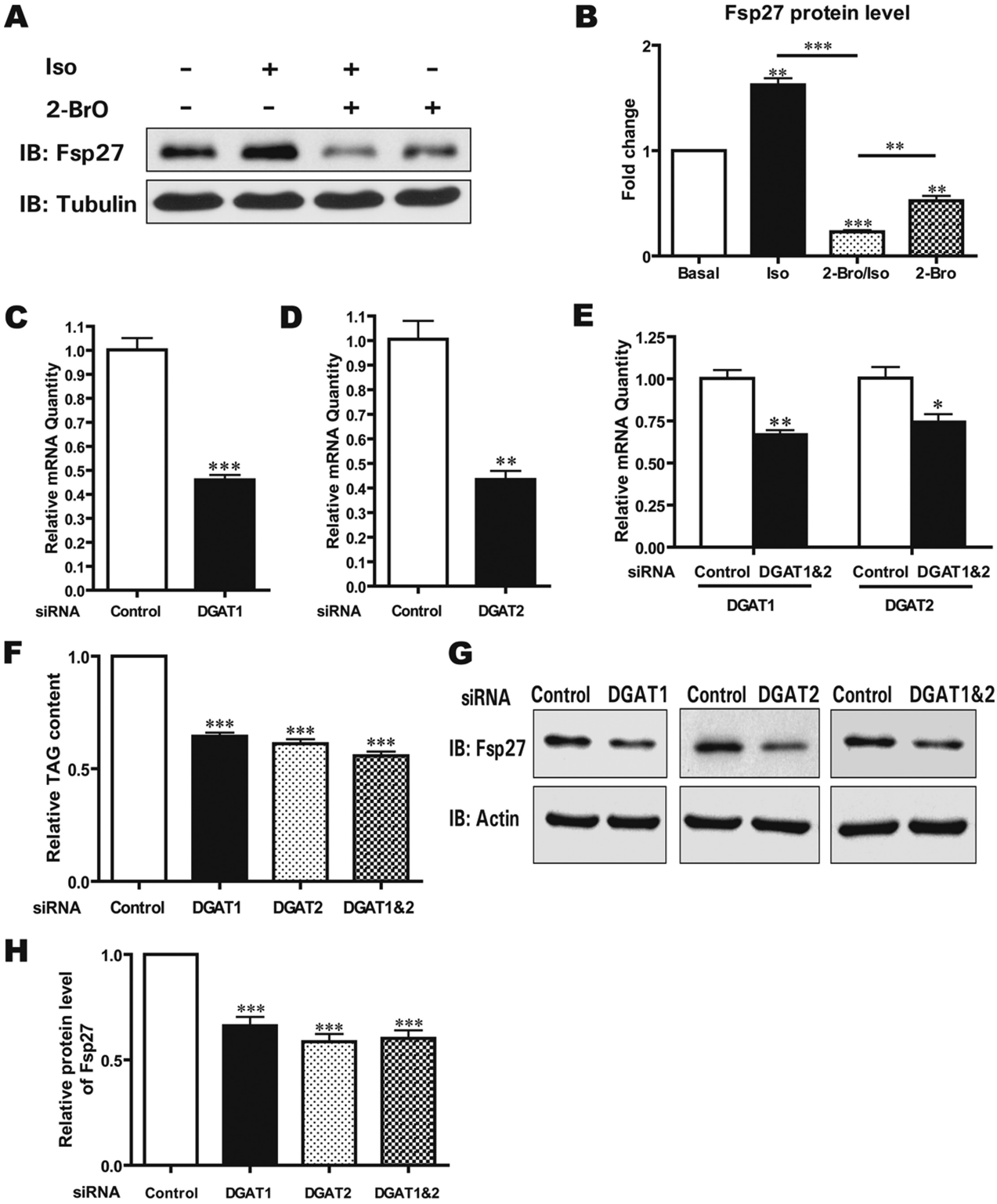

FIGURE 5. **Fsp27 accumulation is dependent on DGAT activity.** *A*, Iso-induced Fsp27 accumulation is dependent on DGAT activity. Differentiated 3T3-L1 adipocytes were treated with Iso alone (*lane 2*), 2-BrO (1.2 mM) alone (*lane 4*), or both (*lane 3*) for 1 h and then harvested to determine the Fsp27 level. *B*, quantitative analysis of the Fsp27 level in *A*. A Student's two-tailed *t* test (unpaired) was used for statistical analysis (***, $p < 0.001$; **, $p < 0.01$, $n = 3$). *C* and *D*, knockdown of DGAT1 or DGAT2 in adipocytes. Differentiated 3T3-L1 adipocytes (5 days after induction) were transfected with 200 nM siRNA specific for DGAT1 or DGAT2 using Lipofectamine 2000. Two days after transfection, total RNA was extracted, and the mRNA level of DGAT1 or DGAT2 was evaluated using quantitative real-time PCR analysis. A Student's two-tailed *t* test (unpaired) was used for statistical analysis (**, $p < 0.01$; ***, $p < 0.001$, $n = 3$). *E*, knockdown of both DGAT1 and DGAT2 in adipocytes. The DGAT1- and DGAT2-specific siRNAs were mixed together and transfected into differentiated 3T3-L1 adipocytes (5 days after induction). Two days after transfection, the mRNA level of DGAT1 and DGAT2 was evaluated as described in *C* and *D*. A Student's two-tailed *t* test (unpaired) was used for statistical analysis (*, $p < 0.05$; **, $p < 0.01$, $n = 3$). *F*, reduced total TAG content in differentiated 3T3-L1 cells following the depletion of DGAT1 and DGAT2 alone or DGAT1 and DGAT2 in combination. Two days after siRNA transfection, total cellular lipids were extracted, and the amount of TAG was evaluated using TLC. A Student's two-tailed *t* test (unpaired) was used for statistical analysis (***, $p < 0.001$, $n = 3$). *G*, Fsp27 accumulation is reduced in DGAT1 and DGAT2 knockdown 3T3-L1 adipocytes. *H*, quantitative analysis of the Fsp27 level from *G*. A Student's two-tailed *t* test (unpaired) was used for statistical analysis (***, $p < 0.001$, $n = 3$).

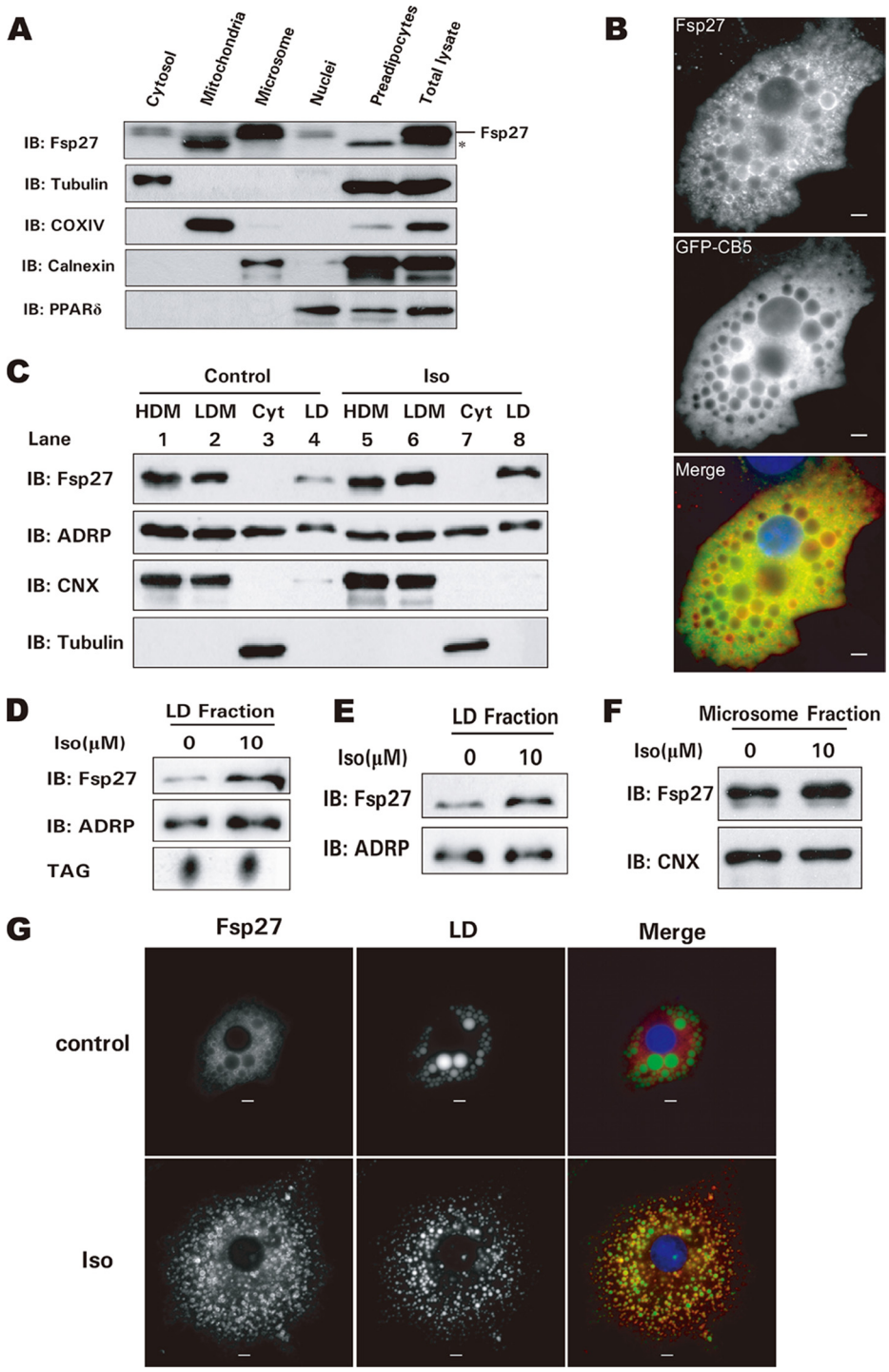

FIGURE 6. **Fsp27 is also localized to the ER, and increased Fsp27 following β-agonist treatment mainly associates with LDs.** *A*, Fsp27 is present in the ER-enriched fraction in differentiated 3T3-L1 adipocytes. A biochemical fractionation experiment was performed using differentiated 3T3-L1 adipocytes (8 days after induction). The same percentage of each sample was loaded onto a SDS-polyacrylamide gel. 3T3-L1 preadipocytes were used as a negative control for Fsp27 expression. *B*, Fsp27 is co-localized with the ER-specific protein CB5 in 3T3-L1 adipocytes. 3T3-L1 adipocytes (7 days after induction) were electroporated with an expression plasmid encoding GFP-CB5. Endogenous Fsp27 was stained using a rabbit anti-Fsp27 antibody (*red*). GFP-CB5 (*green*) was used as an ER marker to visualize the ER network. *Scale bar*, 5 μm. *C*, increased Fsp27 protein level in the LD fraction of Iso (2 h)-treated 3T3-L1 adipocytes. *HDM*, high density microsome; *LDM*, low density microsome; *Cyt*, cytosol. A similar percentage of each fraction was loaded. *D* and *E*, increased Fsp27 protein level in the LD fraction after Iso treatment. The amount of TAG or ADRP was used to normalize sample loading. *F*, Fsp27 accumulation slightly increases in the ER fraction of 3T3-L1 adipocytes after Iso treatment. Calnexin (*CNX*) was used as a specific marker and loading control for the ER fraction. *G*, lipid droplet morphology and enhanced Fsp27 staining signal on the LDs of 3T3-L1 adipocytes in the presence of Iso (2 h). LDs were stained with BODIPY (*green*), and Fsp27 was stained with a rabbit anti-Fsp27 antibody (*red*). *Scale bar*, 5 μm.

namically regulated by lipolysis and fatty acid esterification. We have characterized the critical residues for the control of Fsp27 stability, demonstrating that three lysine residues in the C-terminal region of Fsp27 serve as acceptor sites for its ubiquitination and degradation. Substitution of these lysine residues with alanines led to significantly reduced Fsp27 ubiquitination and increased stability. It has been shown that several other LD-associated proteins, such as ADRP, perilipin, and Cidea, have varying half-lives and are all subjected to the ubiquitin-dependent degradation pathway (13, 25–27). Thus, our current work suggests a general role for ubiquitination-mediated protein degradation in the regulation of LD-associated proteins.

It has been noted that lipid loading by supplementing fatty acids in the culture medium could enhance the accumulation of other LD-associated proteins, including ADRP, perilipin, and caveolin-1 (25, 26, 28, 29). Here, a gradual increase in Fsp27 accumulation in the presence of exogenous fatty acids was also observed in 3T3-L1 adipocytes. Importantly, we observed that Fsp27 stability can be modulated by factors and events that alter the dynamics of lipid synthesis and LD formation. Treatment with a β-agonist that stimulates lipolysis and fatty acid re-esterification in adipocytes resulted in an increased Fsp27 half-life and its rapid accumulation. In addition, the use of medium supplemented with exogenous fatty acids that stimulate TAG synthesis further enhanced β-agonist-induced Fsp27 accumulation. Furthermore, the addition of 2-BrO, which could inhibit DGAT activity and block TAG synthesis, dramatically reduced Fsp27 accumulation and abrogated the effect of the β-agonist on the induction of Fsp27 accumulation. Finally, reduced DGAT1 and DGAT2 expression through siRNA-mediated silencing significantly impaired Fsp27 accumula-

tion. On the other hand, we observed that the stabilization of Fsp27 (*e.g.* the Fsp3K-A mutant or the addition of a proteasome inhibitor) promotes lipid storage and LD formation. Therefore, the availability of free fatty acids in adipocytes appears to be an essential determinant for the stabilization of Fsp27 through promoting TAG synthesis and nascent LD formation. The stabilization of Fsp27 by TAG synthesis and LD formation further enhances lipid storage, providing positive feedback to the regulation of lipid storage in adipocytes. It is likely that, in a metabolic state in adipocytes that lack sufficient fatty acid supply, TAG synthesis and nascent LD formation are reduced, and the majority of Fsp27 translated from the ER may undergo ubiquitin-dependent proteasomal degradation.

Moreover, we observed that Fsp27 with amino acid substitution in the key lysine residues (Fsp3K-A) was able to enhance the stability of endogenous Fsp27 in a dominant fashion and increase lipid storage in differentiated 3T3-L1 adipocytes. The underlying mechanism of such protection is not clear. It is possible that the amount of ubiquitin-conjugating enzyme (E2) or E3 ligase for Fsp27 ubiquitination is limited and that a stable Fsp27, as is the case for Fsp3K-A, was able to compete in the binding of these factors, resulting in less efficient ubiquitination and degradation of endogenous Fsp27. Alternatively, in support of a positive feedback mechanism for the control of Fsp27 stability, the stabilization of endogenous Fsp27 by the Fsp3K-A mutant might be a consequence of enhanced lipid storage, which changes the cell to a state that favors LD formation. Therefore, the regulation of Fsp27 stability in adipocytes provides an interesting mechanism to sense hormonal and metabolic changes, in particular TAG synthesis and dynamic LD formation in adipocytes.

It is unclear how a β-agonist can induce Fsp27 accumulation much faster than supplementation with exogenous fatty acids in the culture medium, because we observed Fsp27 accumulation within half an hour of β-agonist treatment. Yet, increased Fsp27 level was only observed 6 h after OA treatment. One possibility is that β-agonist treatment of adipocytes releases a large amount of free fatty acids that can be rapidly transported to the ER and stimulate TAG synthesis. The increased TAG synthesis in turn stimulates the release of nascent LDs from the ER to the cytosol, resulting in Fsp27 stabilization. Indeed, adipocyte fatty acid-binding protein has been shown to be associated with hormone-sensitive lipase and was co-translocated to LDs after stimulation of lipolysis (30). Furthermore, a previous study has shown that LDs are in close contact with the ER (31). The localization of adipocyte fatty acid-binding protein to LDs and the close contact between the ER and the LDs may facilitate the transport of free fatty acids released during lipolysis to the ER for re-esterification. The mechanism by which TAG synthesis and nascent LD formation in adipocytes stimulate Fsp27 accumulation and enhance its stability is not clear. Because Fsp27 is localized to both the ER and cytosolic LDs and the portion of Fsp27 associated with LDs significantly increased after β-agonist treatment, it is likely that Fsp27 is sequestered from binding to E3 ligase and subsequent ubiquitination is prevented when it is associated with LDs in the cytosol, leading to Fsp27 accumulation on the LDs. In conclusion, we have demonstrated that Fsp27 is a highly regulated protein in adipocytes, because its stability can be controlled by metabolic processes, such as β-agonist stimulation, fatty acid re-esterification, TAG synthesis, and the lipid storage status.

Acknowledgment—We thank members of Peng Li's laboratory in Tsinghua University for technical assistance and helpful discussions.

REFERENCES

1. Gong, J., Sun, Z., and Li, P. (2009) *Curr. Opin. Lipidol.* **20,** 121–126
2. Zhou, Z., Toh, S. Y., Chen, Z., Guo, K., Ng, C. P., Ponniah, S., Lin, S. C., Hong, W., and Li, P. (2003) *Nat. Genet.* **35,** 49–56
3. Li, J. Z., Ye, J., Xue, B., Qi, J., Zhang, J., Zhou, Z., Li, Q., Wen, Z., and Li, P. (2007) *Diabetes* **56,** 2523–2532
4. Egan, J. J., Greenberg, A. S., Chang, M. K., Wek, S. A., Moos, M. C., Jr., and Londos, C. (1992) *Proc. Natl. Acad. Sci. U.S.A.* **89,** 8537–8541
5. Brasaemle, D. L., Dolios, G., Shapiro, L., and Wang, R. (2004) *J. Biol. Chem.* **279,** 46835–46842
6. Puri, V., Konda, S., Ranjit, S., Aouadi, M., Chawla, A., Chouinard, M., Chakladar, A., and Czech, M. P. (2007) *J. Biol. Chem.* **282,** 34213–34218
7. Keller, P., Petrie, J. T., De Rose, P., Gerin, I., Wright, W. S., Chiang, S. H., Nielsen, A. R., Fischer, C. P., Pedersen, B. K., and MacDougald, O. A. (2008) *J. Biol. Chem.* **283,** 14355–14365
8. Yu, S., Matsusue, K., Kashireddy, P., Cao, W. Q., Yeldandi, V., Yeldandi, A. V., Rao, M. S., Gonzalez, F. J., and Reddy, J. K. (2003) *J. Biol. Chem.* **278,** 498–505
9. Viswakarma, N., Yu, S., Naik, S., Kashireddy, P., Matsumoto, K., Sarkar, J., Surapureddi, S., Jia, Y., Rao, M. S., and Reddy, J. K. (2007) *J. Biol. Chem.* **282,** 18613–18624
10. Matsusue, K., Kusakabe, T., Noguchi, T., Takiguchi, S., Suzuki, T., Yamano, S., and Gonzalez, F. J. (2008) *Cell Metab.* **7,** 302–311
11. Nishino, N., Tamori, Y., Tateya, S., Kawaguchi, T., Shibakusa, T., Mizunoya, W., Inoue, K., Kitazawa, R., Kitazawa, S., Matsuki, Y., Hiramatsu, R., Masubuchi, S., Omachi, A., Kimura, K., Saito, M., Amo, T., Ohta, S., Yamaguchi, T., Osumi, T., Cheng, J., Fujimoto, T., Nakao, H., Nakao, K., Aiba, A., Okamura, H., Fushiki, T., and Kasuga, M. (2008) *J. Clin. Invest.* **118,** 2808–2821
12. Toh, S. Y., Gong, J., Du, G., Li, J. Z., Yang, S., Ye, J., Yao, H., Zhang, Y., Xue, B., Li, Q., Yang, H., Wen, Z., and Li, P. (2008) *PLoS ONE* **3,** e2890
13. Chan, S. C., Lin, S. C., and Li, P. (2007) *Biochem. J.* **408,** 259–266
14. Qi, J., Gong, J., Zhao, T., Zhao, J., Lam, P., Ye, J., Li, J. Z., Wu, J., Zhou, H. M., and Li, P. (2008) *EMBO J.* **27,** 1537–1548
15. Dull, T., Zufferey, R., Kelly, M., Mandel, R. J., Nguyen, M., Trono, D., and Naldini, L. (1998) *J. Virol.* **72,** 8463–8471
16. Suzuki, R., Tobe, K., Aoyama, M., Sakamoto, K., Ohsugi, M., Kamei, N., Nemoto, S., Inoue, A., Ito, Y., Uchida, S., Hara, K., Yamauchi, T., Kubota, N., Terauchi, Y., and Kadowaki, T. (2005) *J. Biol. Chem.* **280,** 3331–3337
17. Joost, H. G., and Schürmann, A. (2001) *Methods Mol. Biol.* **155,** 77–82
18. Londos, C., Brasaemle, D. L., Schultz, C. J., Adler-Wailes, D. C., Levin, D. M., Kimmel, A. R., and Rondinone, C. M. (1999) *Ann. N.Y. Acad. Sci.* **892,** 155–168
19. Brasaemle, D. L., Levin, D. M., Adler-Wailes, D. C., and Londos, C. (2000) *Biochim. Biophys. Acta* **1483,** 251–262
20. Mayorek, N., and Bar-Tana, J. (1985) *J. Biol. Chem.* **260,** 6528–6532
21. Kuerschner, L., Moessinger, C., and Thiele, C. (2008) *Traffic* **9,** 338–352
22. Croze, E. M., and Morré, D. J. (1984) *J. Cell. Physiol.* **119,** 46–57
23. Puri, V., Ranjit, S., Konda, S., Nicoloro, S. M., Straubhaar, J., Chawla, A., Chouinard, M., Lin, C., Burkart, A., Corvera, S., Perugini, R. A., and Czech, M. P. (2008) *Proc. Natl. Acad. Sci. U.S.A.* **105,** 7833–7838
24. Ye, J., Li, J. Z., Liu, Y., Li, X., Yang, T., Ma, X., Li, Q., Yao, Z., and Li, P.

(2009) *Cell Metab* **9,** 177–190
25. Xu, G., Sztalryd, C., Lu, X., Tansey, J. T., Gan, J., Dorward, H., Kimmel, A. R., and Londos, C. (2005) *J. Biol. Chem.* **280,** 42841–42847
26. Xu, G., Sztalryd, C., and Londos, C. (2006) *Biochim. Biophys. Acta* **1761,** 83–90
27. Kovsan, J., Ben-Romano, R., Souza, S. C., Greenberg, A. S., and Rudich, A. (2007) *J. Biol. Chem.* **282,** 21704–21711
28. Brasaemle, D. L., Barber, T., Kimmel, A. R., and Londos, C. (1997) *J. Biol. Chem.* **272,** 9378–9387
29. Orlicky, D. J., Degala, G., Greenwood, C., Bales, E. S., Russell, T. D., and McManaman, J. L. (2008) *J. Cell Sci.* **121,** 2921–2929
30. Smith, A. J., Sanders, M. A., Thompson, B. R., Londos, C., Kraemer, F. B., and Bernlohr, D. A. (2004) *J. Biol. Chem.* **279,** 52399–52405
31. Szymanski, K. M., Binns, D., Bartz, R., Grishin, N. V., Li, W. P., Agarwal, A. K., Garg, A., Anderson, R. G., and Goodman, J. M. (2007) *Proc. Natl. Acad. Sci. U.S.A.* **104,** 20890–20895